Numerical Investigation into Trapezoid Surface Texture of Journal Bearing and RBD Palm Oil as Lubricant

Rasep, Zuraidah
School of Mechanical Engineering, Faculty of Engineering, Universiti Teknologi Malaysia

Muhammad Noor Afiq Witri Muhammad Yazid
School of Mechanical Engineering, Faculty of Engineering, Universiti Teknologi Malaysia

Samion, Syahrullail
School of Mechanical Engineering, Faculty of Engineering, Universiti Teknologi Malaysia

Nor Azwadi Che Sidik
Department of Mechanical Precision Engineering, Malaysia-Japan International Institute of Technology, Universiti Teknologi Malaysia

https://doi.org/10.5109/7183451

出版情報：Evergreen. 11 (2), pp.1389-1398, 2024-06. 九州大学グリーンテクノロジー研究教育センター
バージョン：

Numerical Investigation into Trapezoid Surface Texture of Journal Bearing and RBD Palm Oil as Lubricant

Zuraidah Rasep[1,2,*], Muhammad Noor Afiq Witri Muhammad Yazid[1], Syahrullail Samion[1], Nor Azwadi Che Sidik[3]

[1] School of Mechanical Engineering, Faculty of Engineering, Universiti Teknologi Malaysia, 81310 UTMSkudai, Johor, Malaysia.

[2] Process Engineering Technology Section, Malaysian Institute of Chemical and Bioengineering Technology (MICET), Universiti Kuala Lumpur, Lot 1988, Taboh Naning, 78000 Alor Gajah, Melaka, Malaysia.

[3] Department of Mechanical Precision Engineering, Malaysia-Japan International Institute of Technology, Universiti Teknologi Malaysia, Jalan Sultan Yahya Petra, 54100 Kuala Lumpur, Malaysia.

*Author to whom correspondence should be addressed:
E-mail: zuraidahr@unikl.edu.my

(Received June 15, 2022; Revised March 11, 2024; Accepted June 14, 2024).

Abstract: Researchers are interested in changing the surface texture of journal bearings to potentially improve their performance. This study investigates the use of RBD palm oil as a lubricant in journal bearings with various surface textures. The research focuses on different geometric shapes, such as square (geometry 1) and trapezoid (geometries 2 and 3), located in the divergent A area. Results show that geometry 1 enhances journal bearing performance at 800 and 1000 rpm, while geometry 3 (trapezoid) improves performance specifically at 1000 rpm with a constant eccentricity ratio of 0.7.

Keywords: Palm oil, Journal bearing, CFD, ANSYS FLUENT, Tribology, Surface texture

1. Introduction

An environmentally sustainable lubricant, vegetable oil possesses qualities that make it adaptable for use across various industries requiring lubrication, with minor modifications. Studies have highlighted unique characteristics of vegetable oil, seldom found in mineral oil, rendering it highly advantageous for industrial use. Nevertheless, challenges such as inadequate performance in low temperatures and susceptibility to oxidation present hurdles for its widespread application [1)]. For instance, a case study conducted by [2)] examined the tribological performance of a nanofluid derived from modified jatropha oil, a non-edible source, augmented with activated carbon nanoparticles. Additionally, [3)] investigated the potential of jatropha oil and demonstrated its superior lubricating capabilities in reducing friction and wear compared to lubricants based on engine and hydraulic oils.

According to [4)], palm oil stands out as the preferred vegetable oil due to its notably low coefficient of friction compared to alternatives like sunflower oil, rapeseed oil, and soybean oil. [5)] also propose that blending mineral oil with vegetable oil can enhance its effectiveness. An instance of palm oil application in industry involves the structural modification of palm stearin through catalyst introduction. Candida antarctica lipase improves both physicochemical and tribological properties, showcasing palm stearin-derived lubricant as a promising base stock due to its favorable biodegradability and tribological traits [6)]. In the subsequent study,[7)] utilized crude fatty acids as lubricants in cold forward extrusions, resulting in reduced process load. They characterized fatty acids as effective in reducing friction between the billet and die surfaces, providing robust protection as piston stroke increases. Later [8)] introduced graphene nanoparticles into vegetable oil at concentrations of 25 ppm, 50 ppm, and 100 ppm, leading to notable improvements in tribological properties by reducing wear scar diameter and friction coefficient.[9)] emphasized in their paper that base oils often fail to withstand various operating conditions, prompting the formulation and blending of appropriate additives to enhance the tribological properties of chosen lubricants for specific applications. Meanwhile, [10)] stated that the performance of RBD (refined bleached and deodorized) palm stearin rivals that of paraffinic mineral oil in reducing frictional constraints in cold work extrusion processes. Additionally, [11)] demonstrated that blending palm oil with tertiary-butyl-hydroquinone can exhibit antioxidant properties, thereby reducing friction and wear.

Furthermore, [12] suggested further investigation into the potential of nano-lubricants on tribological performance through theoretical and experimental analyses. [13] discovered that compared to CMFO (commercial metal forming oil), RBD palm kernel oil exhibited superior performance in terms of surface roughness. This finding was corroborated by [14] , who revealed that the anti-friction and anti-wear properties of PFAD (palm fatty acid distillate) surpassed those of engine and hydraulic mineral oils. Subsequent studies by [15] and [16] confirmed that RBD palm olein delivers satisfactory lubrication performance in cold work metal forming processes, suggesting its potential as a partial bio-lubricant due to its low wear and effective bio-lubrication performance.

In a study by [17], researchers demonstrated that employing RBD palm oil as a dielectric fluid enhances machining performance. Furthermore, [18] investigated the energy-water nexus in palm oil biodiesel production, encompassing processes from plantation to palm oil processing into CPO (crude palm oil), and biodiesel production from CPO. Lastly, [19] discovered that at lower loads, PMO (palm mid olein) exhibited a higher maximum pressure than SAE 40. Additionally, they found that increasing radial load led to an increase in maximum pressure. Two years later, the same author [20] further revealed that PMO displays superior thermal resistivity compared to SAE 40. Moreover, PMO exhibited a lower friction coefficient across all testing conditions.

Surface texturing has emerged as a promising avenue for enhancing the tribological characteristics of hydrodynamic journal bearings, offering potential contributions to green tribology, as suggested by [21]. For instance, [22] conducted a case study comparing non-textured bearings to dimple-textured journal bearings with axial grooves, revealing that the latter exhibited a higher dimensionless load-carrying capacity. Subsequently, [23] [24] found that incorporating a partial groove along the 90°-180° region of the bearing surface resulted in significant increases of 81.9 percent in maximum fluid film pressure and 75.9 percent in load-carrying capacity compared to a smooth journal bearing surface, with no additional frictional power loss or torque. Researchers in this field have proposed important considerations as guidelines to enhance journal bearing performance. According to [25], the optimal design of the textured area depends heavily on geometrical parameters and operating conditions. [26] emphasized the importance of texture depth, location, and number in achieving the greatest improvement in bearing stability during design. [27] found that textures near the lubricant inlet area enhance bearing performance, with shallow dimples outperforming deep ones. Additionally, [28] noted that surface textures affect the eccentricity ratio of a journal bearing, with the position and area covered by the textured region significantly impacting performance. The physical mechanism of surface texture is influenced by both positive and negative hydrodynamic effects caused by the geometrical structure. [21] asserted that a partially textured bearing with appropriate geometry and location tends to be more stable. Furthermore, lubricant viscosities play a crucial role in evaluating overall machine performance. For example, [29] investigated various types and viscosities of lubricants used in heat pump cycles to understand their effects on heat pump performance. Consequently, temperature-dependent viscosity was considered in the CFD ANSYS FLUENT system in this study.

Various geometries have been explored in surface texture modification of journal bearings. For instance, the chevron geometry was examined by both [26] and [30]. Spherical geometry was studied by [31] and [25], while square dimple geometry was investigated by [32] and [33]. Triangular and cylindrical geometries were explored by [34] and [35] , respectively. Furthermore, groove geometry was analyzed by [36], while [24] focused on partial groove geometry. Some researchers have delved into multiple types of geometries in their surface texture modification case studies. For example, [37] examined square, cylindrical, and triangular geometries, while [21] investigated circular, square, and densely distributed square textures, along with micro-spherical and cylindrical dimples as studied by Guo [22]. Additionally, Yu and colleagues [38] explored the geometries of spheroid1 (S1), spheroid2 (S2), sphere (Sp), triangle (T), and groove (G). An innovative approach in surface texture modification of journal bearings involves compound textures, which combine two geometries. For example, [39] studied compound dimples (spherical and rectangular) along with dimples with rectangular geometry. Three years later, Meng and Zhang [40] investigated the effects of introducing surface texture, specifically compound texture (rectangle semicircle cross-section) and simple texture (rectangle cross-section), on journal bearing performance. Moreover, as highlighted by [4] , the challenge in journal bearing surface texture modification lies in selecting the best parameters and geometry to optimize performance. Additionally, Computational Fluid Dynamics (CFD) is preferred over experimental methods for such analyses.

CFD, a computational technique utilizing computational tools, is applied to solve fluid flow and its governing equations numerically. This involves converting these equations into a set of linear equations and solving them iteratively. CFD is widely used across various industries, including aerodynamics, biomedical engineering, combustion, drying, heat exchangers, HVAC systems, hydropower, power plants, reactors, transportation, wind power, and more. In this case study, numerical analysis was chosen to examine the surface texture modification of journal bearings. The simulation was performed using the CFD software ANSYS FLUENT. Previous research has shown that employing the commercial CFD software FLUENT 14.0 significantly enhances the performance of grease-lubricated journal bearings with surface texture when used as an analytical method [38].

Until now, there hasn't been thorough investigation into utilizing trapezoid surface texture for textured journal bearings. Additionally, RBD palm oil presents a promising alternative due to its environmentally friendly properties compared to traditional engine oil. Hence, this paper aims to evaluate the feasibility of implementing trapezoid surface texture in journal bearings through a simulation approach using CFD ANSYS FLUENT and RBD palm oil as the lubricant.

2. Methodology

The initial stage of the methodology involves validation, where experimental data is used as a benchmark to initiate the simulation study using CFD ANSYS FLUENT, as shown in Fig. 1. The process in CFD ANSYS FLUENT begins with creating the journal bearing in the design modeler, followed by meshing, selection of appropriate boundary conditions, and specification of key parameters in the FLUENT section. Finally, all results and contours can be visualized in the post-processing stage. The validation process has been conducted and documented. A comparison of data was carried out between the experimental work and the current study through simulation at a rotational speed of 1500 rpm and an eccentricity ratio of 0.8 [42) 43)].

The discrepancy between both methods was determined to be 12.0%. Consequently, the simulation method validated using experimental data will be utilized in all subsequent simulation studies.

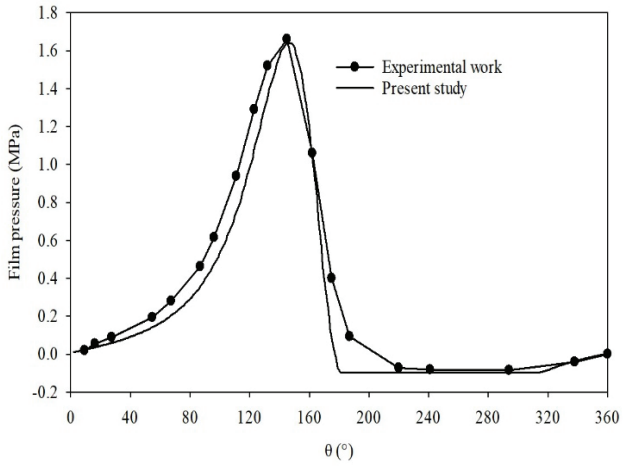

Fig. 1: Comparing the present case study utilizing CFD ANSYS FLUENT with experimental work by [35].

Table 2 provides a comprehensive overview of the parameters employed in both the experimental investigation and numerical analysis. Notably, the rotational speed is capped at a maximum of 1000 rpm, a decision informed by the recommendation cited in [44)]. his precautionary measure stems from observations in a pertinent thesis, which underscored limiting the journal bearing's operational speed to 1000 rpm, despite the machine's capacity of 1500 rpm. The rationale behind this choice primarily revolves around preempting potential vibration issues that could manifest when subjecting the journal bearing rig to elevated rotational speeds during data collection. Furthermore, the selection of an eccentricity ratio of 0.7 is grounded in the guidance provided by [42)] , which posits that maintaining the eccentricity ratio within the range of 0.8 to 0.9 results in a narrower positive pressure peak. This choice is paramount to mitigate stress concentration within the bearing system. Additionally, empirical observations suggest that operating the plain bearing under conditions where the eccentricity ratio is too low, such as 0.4 or 0.5, may yield insufficient pressure to effectively separate the journal surface from the bearing surface. Consequently, during the design phase of a plain bearing, it is imperative to opt for an eccentricity ratio of 0.6 or 0.7 to ensure optimal performance and longevity of the system.

Parameter	Value
Eccentricity ratio	0.7
Attitude angle	49^0
Rotational speed (rpm)	200, 400, 600, 800, and 1000
Bearing inner radius (mm)	40.041
Shaft radius (mm)	40.001
Bearing length (mm)	80.21
Radial clearance (mm)	0.04
Length-diameter ratio	1.0

Table 1. Parameters used for both experimental study and numerical analysis.

The investigation explored various eccentricity ratios at 0.7 and rotational speeds from 200 rpm to 1000 rpm in 200 rpm increments. Figure 5 compares maximum fluid film pressure between engine oil and RBD palm oil under constant viscosity conditions. Unlike previous studies, a cavitation model was consistently employed in this case study for enhanced accuracy in load-carrying predictions and vortex formation, as highlighted in references [45)] and [43)]. Mesh independence analysis utilized a structural mesh with specific divisions: 110 along the circumferential direction, 6 through the fluid film thickness, and 20 axially.

Figure 2 depicts the placement of surface texture at both the divergent and convergent areas of the journal bearing, with a rough sketch of the journal bearing's scale provided. The division into divergent and convergent areas was determined based on the minimum film thickness of the journal bearing. Additionally, Figure 3 exhibits various geometry shapes, including Geometry 1 (a trapezoid), Geometry 2 (another trapezoid), and Geometry 3, all situated within divergent A.

Boundary conditions were carefully specified for this study. One side of the lubricating film clearance was marked as the inlet, while the opposite side was designated as the outlet, devoid of any holes, as depicted in Fig. 4. The inlet side was characterized as a pressure inlet, whereas the outlet was labeled as a pressure outlet. A stationary wall was assigned to the inner surface of the bearing, while a moving wall was allocated to the outer

surface of the shaft or journal.

Conjugate heat transfer and cavitation models were employed in this case study. Specifically, the Zwart Gerber Belamri model was selected for cavitation modeling in the simulation performed with CFD ANSYS FLUENT. The fluid flow was assumed to be laminar, and gravitational effects were disregarded.

Inlet and outlet temperatures were set at 400K and 410K, respectively. Concerning the fluid properties of RBD palm oil, its density was determined to be 880 kg/m^3, and a temperature-dependent viscosity model was integrated into the system. The viscosity was correlated with temperature using the equation: viscosity = 47.451 * exp (-0.021 * Temperature).

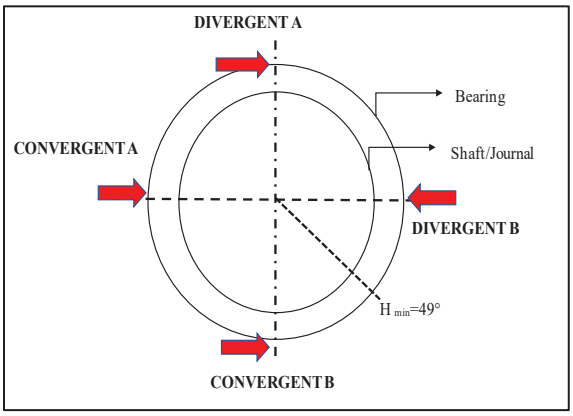

Fig. 2: The surface texture is positioned at both the divergent and convergent areas of the journal bearing. The sketch roughly represents the scale of the journal bearing.

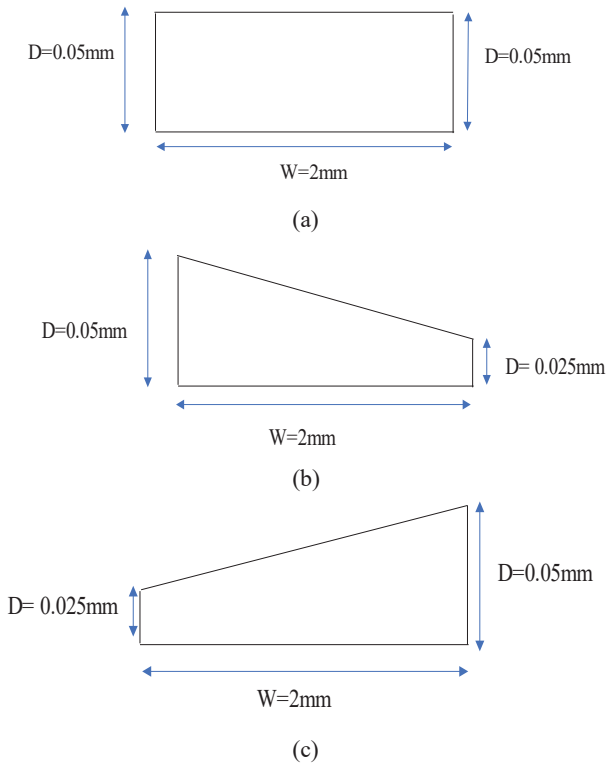

Fig. 3: (a) Shape of geometry 1 and location at divergent A (b) Shape of a trapezoid (geometry 2) and the location at divergent A (c) Shape of a trapezoid (geometry 3) and the location at divergent A.

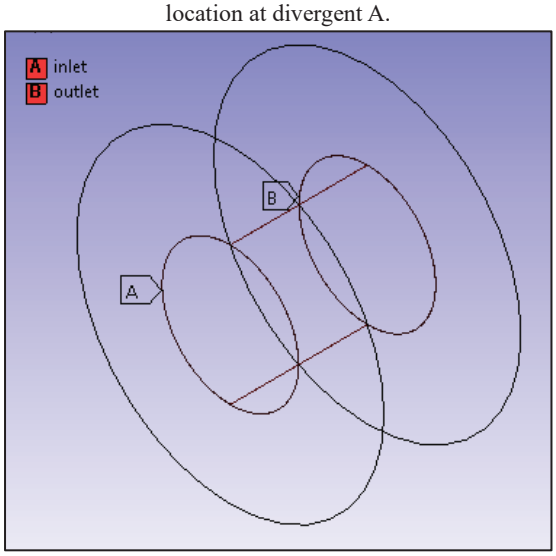

Fig. 4: Boundary condition location for inlet and outlet.

3. Result and discussion

Figure 5 displays a comparison between the maximum fluid film pressures of engine oil and RBD palm oil under constant viscosity conditions, with a rotational speed set at 1000 rpm and an eccentricity ratio of 0.7. The maximum fluid film pressure for engine oil registers at 45.3 MPa, whereas for RBD palm oil, it is 27.5 MPa. This comparison underscores the potential of RBD palm oil as a promising alternative to engine oil, particularly under conditions of constant viscosity. [35] notes that higher rotation speeds lead to lower friction coefficients and quicker temperature buildup. Thus, for subsequent simulation studies, the consideration of temperature buildup was integrated. Another study incorporated conjugate heat transfer and temperature-dependent viscosity, as research suggests that the viscosity of the journal bearing varies with increasing temperature.

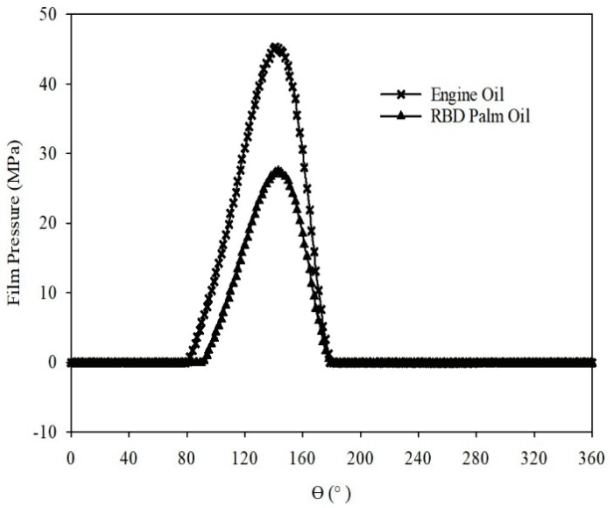

Fig. 5: The comparison between the maximum fluid film pressures of engine oil and RBD palm oil was carried out under

constant viscosity conditions, with a rotational speed of 1000 rpm and an eccentricity ratio of 0.7.

Figure 6 compares a plain bearing with different surface texture modifications for RBD palm oil, considering temperature-dependent viscosity and conjugate heat transfer at 1000 rpm and a 0.7 eccentricity ratio. The results reveal that surface texture at divergent A enhances maximum fluid film pressure compared to a plain journal bearing. Additionally, comparisons were made with other locations such as convergent A, convergent B, and divergent area B. In the convergent field, hydrodynamic pressure effectively separates the bearing from the journal within the fluid film, maintaining consistent fluid properties. However, as the fluid transitions into the divergent field, pressure gradually decreases until reaching saturation, leading to cavitation if the pressure drops below the saturation oil vapor pressure, as outlined in reference [46].

Additionally, [47] demonstrated that the most significant enhancement in journal bearing efficiency occurred at an eccentricity ratio of approximately 0.6, especially when the second angular part of the bearing, surpassing 180°, was textured in the decreasing pressure area, identified as the divergent region in the study. Figure 7 compares the load-carrying capacity (in kN) between a plain bearing and various surface texture modifications for RBD palm oil, factoring in temperature-dependent viscosity and conjugate heat transfer at 1000 rpm and a 0.7 eccentricity ratio. The load-carrying capacity at the divergent A location surpasses that of the plain journal bearing, measuring 11.4 kN, whereas for the plain journal bearing, it stands at 11.2 kN.

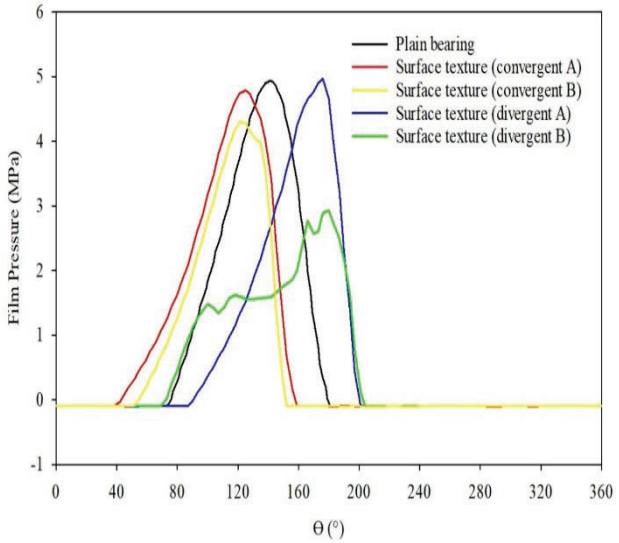

Fig. 6: Comparing a plain bearing with various locations of surface texture modification for RBD palm oil, considering temperature-dependent viscosity, at 1000 rpm and a 0.7 eccentricity ratio.

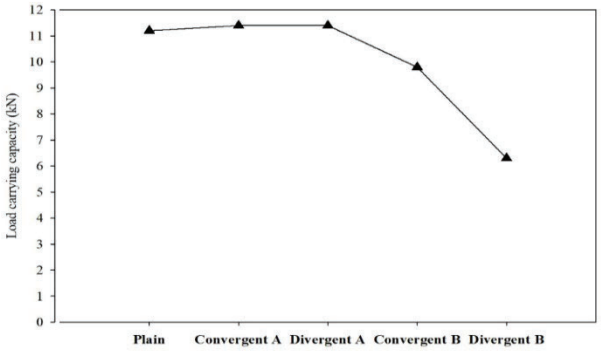

Fig. 7: Comparing the load-carrying capacity (kN) between a plain bearing and different locations of surface texture modification for RBD palm oil, considering temperature-dependent viscosity, at 1000 rpm and a 0.7 eccentricity ratio.

Figure 8 compares a plain journal bearing with Geometry 1, Geometry 2, and Geometry 3 at the location of surface texture (divergent A), considering cavitation and conjugate heat transfer alongside temperature-dependent viscosity at rotational speeds ranging from 200 rpm to 1000 rpm. Figures 8 (a), 8 (b), and 8 (c) consistently show lower maximum fluid film pressure for all Geometry configurations compared to the plain journal bearing. Higher fluid film maximum pressure indicates better load capacity of the journal bearing, which is desirable for optimal performance. However, slight variations are observed, particularly at rotational speeds of 800 rpm and 1000 rpm (Fig. 5 (d) and 5 (e)), where Geometry 1 and Geometry 3 exhibit higher maximum fluid film pressure compared to the plain bearing. Table 2 offers a detailed comparison of maximum fluid film pressure (in MPa) for the plain bearing and different geometries at divergent A across various rotational speeds under a constant eccentricity ratio of 0.7.

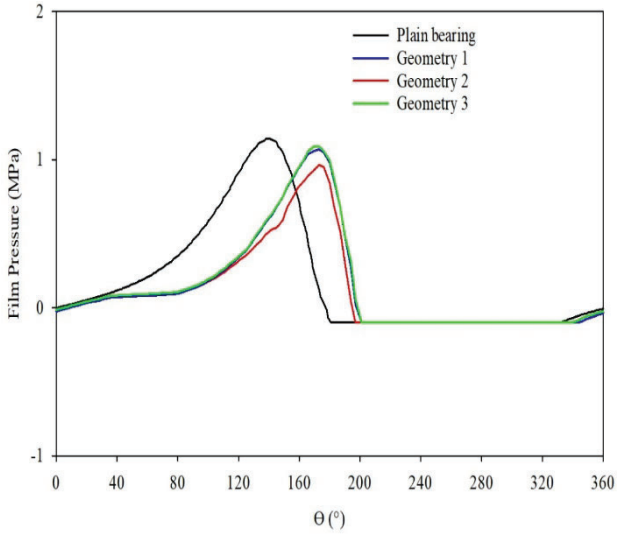

(a)

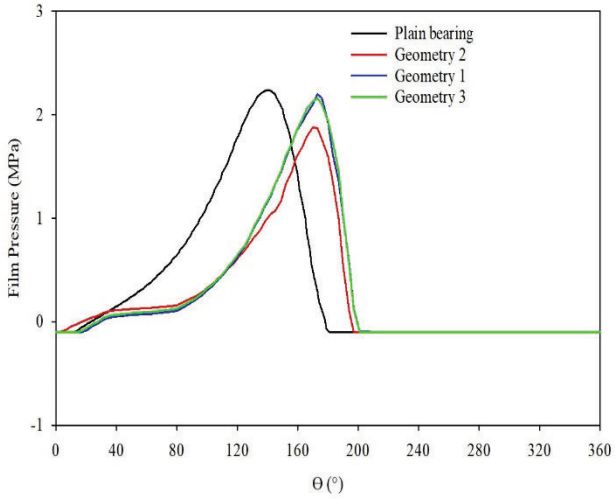

(b)

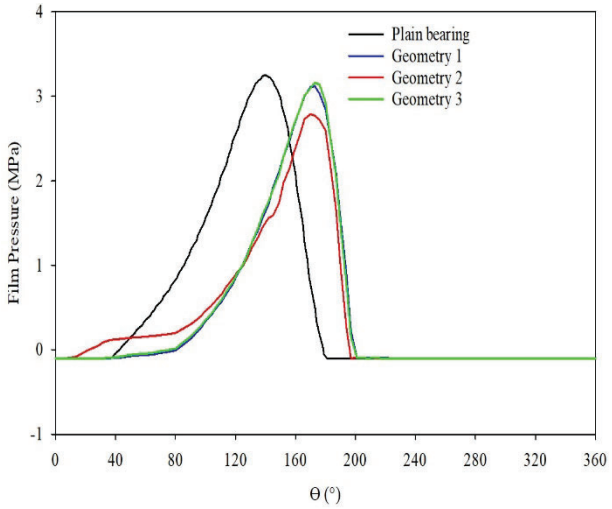

(c)

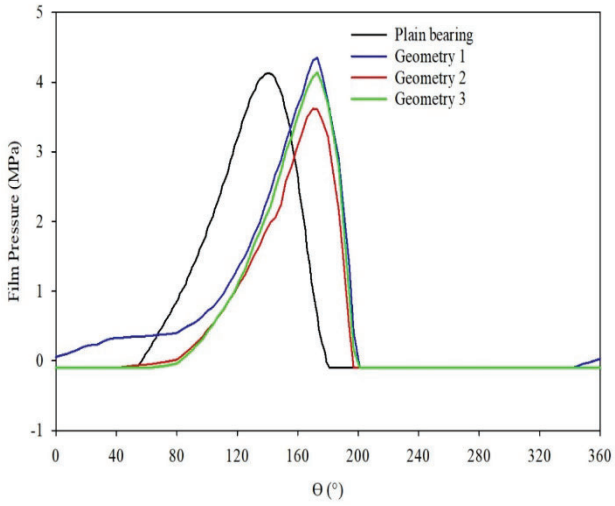

(d)

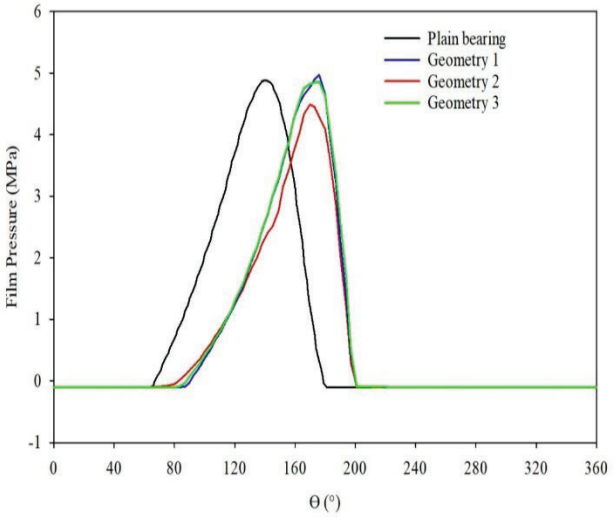

(e)

Fig. 8: Comparison between plain bearing and geometry 1, geometry 2, and geometry 3 at the location of surface texture (divergent A) considering temperature-dependent viscosity at a) 200 rpm, b) 400 rpm, c) 600 rpm, d) 800 rpm and e) 1000 rpm.

Table 2. Comparison of maximum pressure of fluid film (MPa) for plain bearing, geometry 1, geometry 2, and geometry 3 at the location of divergent A at different speeds of journal bearing (200, 400, 600, 800, and 1000 rpm) and constant eccentricity ratio 0.7.

Speed	**The Geometry of Surface Texture**			
(rpm)	**Plain bearing**	**Geometry 1**	**Geometry 2**	**Geometry 3**
	Pmax (MPa)			
200	1.14	1.07	0.97	1.09
400	2.24	2.20	1.88	2.16
600	3.25	3.12	2.79	3.16
800	4.13	4.35	3.62	4.17
1000	4.88	4.97	4.49	4.94

Figure 9 illustrates a contour of the maximum pressure for the fluid film (in MPa), comparing the plain bearing with Geometry 1 at a rotational speed of 800 rpm and an eccentricity ratio of 0.7. Conversely, Figure 10 presents a comparison contour of the maximum pressure for the fluid film (in MPa) among the plain bearing, Geometry 1, and Geometry 3 at a rotational speed of 1000 rpm and an eccentricity ratio of 0.7. These contours are chosen based on the maximum pressure of the fluid film, which demonstrates higher values compared to the plain journal bearing.

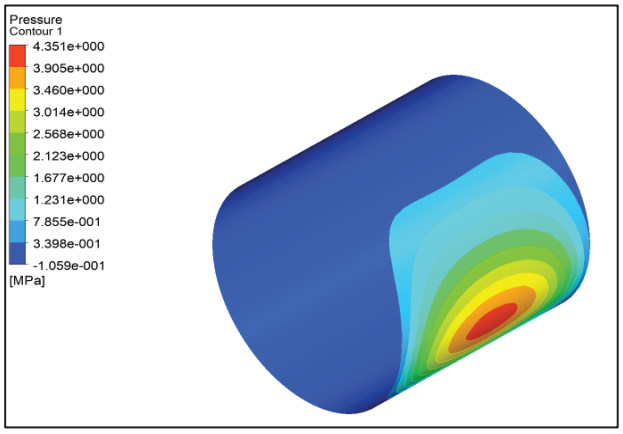

(a)

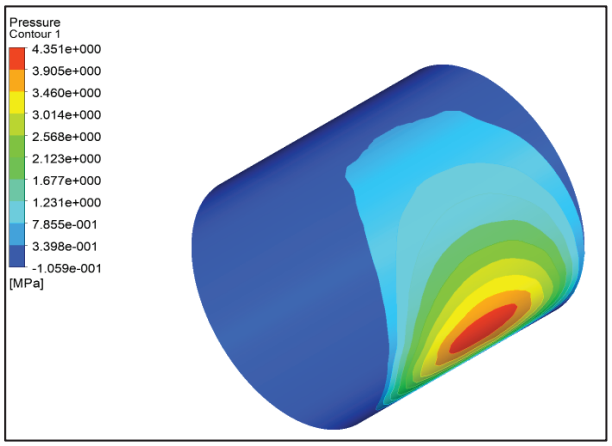

(b)

Fig. 9: Comparison contour of maximum pressure for the fluid film (MPa) between a) plain bearing and b) geometry 1 at a rotational speed of journal bearing 800 rpm and eccentricity ratio 0.7.

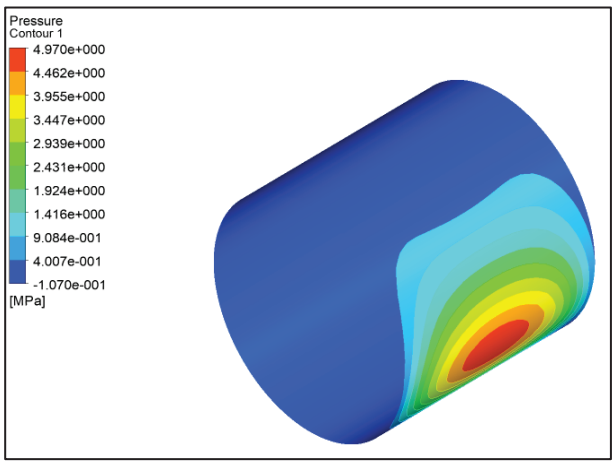

(a)

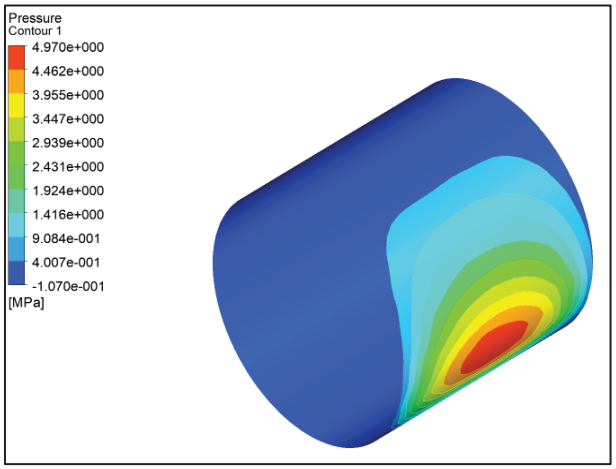

(b)

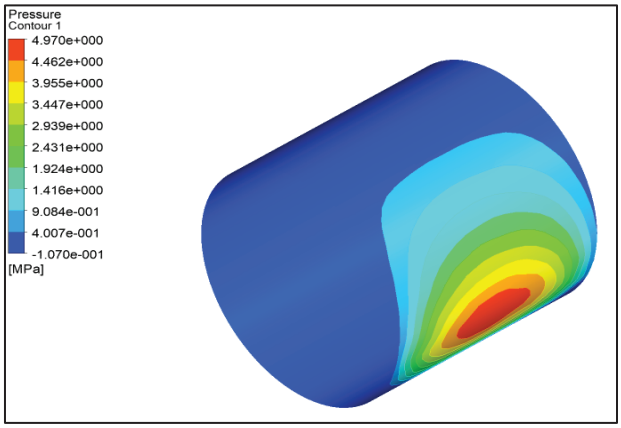

(c)

Fig. 10: Comparison contour of maximum pressure for the fluid film (MPa) between a) plain bearing, b) geometry 1 and c) geometry 3 at a rotational speed of journal bearing 1000 rpm and eccentricity ratio 0.7.

Figure 11 compares the load-carrying capacities (in kN) of a plain bearing with Geometry 1, Geometry 2, and Geometry 3 at the surface texture location (divergent A). This comparison considers temperature-dependent viscosity and conjugate heat transfer at a constant eccentricity ratio of 0.7 and various rotational speeds ranging from 200 rpm to 1000 rpm. The analysis reveals that at 800 rpm, Geometry 1 shows an improvement in load-carrying capacity, measuring 10.1 kN compared to 9.8 kN for the plain bearing. Similarly, at 1000 rpm, both Geometry 1 and Geometry 3 exhibit enhancements in load-carrying capacity, measuring 11.4 kN each, compared to 11.2 kN for the plain bearing.

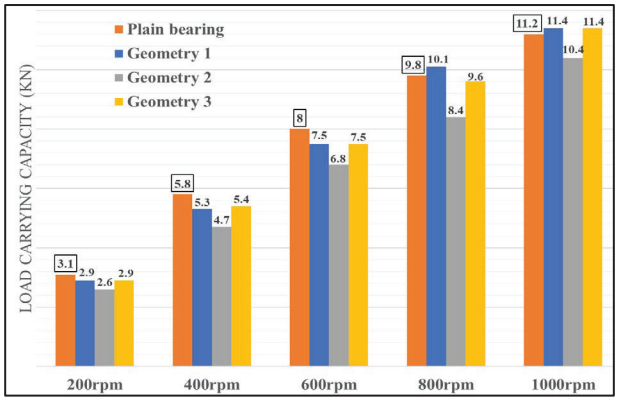

Fig. 11: Load-carrying capacity (kN) comparison between plain bearing and geometry 1, geometry 2, and geometry 3 at the location of surface texture (divergent A) considering temperature-dependent viscosity at 200 rpm,400 rpm,600 rpm, 800 rpm and 1000 rpm.

4. Conclusions

This study investigates the potential of using trapezoid surface texture on journal bearings with RBD palm oil as a lubricant, employing simulation with CFD ANSYS FLUENT. RBD palm oil, a renewable lubricant source, shows promise for future applications. The research serves as a benchmark for incorporating renewable sources into journal bearing surface texture modifications. Key findings indicate that RBD palm oil, in combination with surface texture modifications, particularly at the divergent A area using Geometry 1 shape at rotational speeds of 800 rpm and 1000 rpm, and Trapezoid Geometry 3 shape at 1000 rpm, offers significant improvements over the plain bearing. Geometry 1 at the divergent A area emerges as the optimal choice, demonstrating enhanced performance at both rotational speeds compared to the plain bearing.

Acknowledgments

The authors would like to express their thanks to the Ministry of Higher Education of Malaysia for the FRGS Grant (FRGS/1/2018/TK03/UTM/02/14), Universiti Teknologi Malaysia (UTM) for the Research University Grant (21H50), TDR Grant (05G23) and FRGS Grant (5F074, 5F173). The authors also like to thank Malaysia-Japan International Institute of Technology (MJIIT) and Takasago Thermal Engineering for funding this work under the grant R.K130000.7343.4B472.

References

1) M.A. Dandan, W.M.A.W. Yahaya, S. Samion, and M.N. Musa, “A comprehensive review on palm oil and the challenges using vegetable oil as lubricant base-stock,” *Journal of Advanced Research in Fluid Mechanics and Thermal Sciences.*, 2 (2) 182–197 (2018).

2) N. Talib, N.A. Jamaluddin, T.K. Sheng, L.W. Kiow, H. Abdullah, S. Ahmad, and A. Saleh, “Tribological study of activated carbon nanoparticle in nonedible nanofluid for machining application,” *EVERGREEN Joint Journal of Novel Carbon Resource Sciences & Green Asia Strategy.,* 8 (*2*) 454–460 (2021). doi:10.5109/4480728.

3) I. Golshokouh, M. Golshokouh, F.N. Ani, E. Kianpour, and S. Syahrullail, “Investigation of physical properties for jatropha oil in different temperature as lubricant oil,” *Life Science Journal.*, 10 (8s) 110–119 (2013).

4) Z. Rasep, M.N.A.W.M. Yazid, and S. Samion, “Lubrication of textured journal bearing by using vegetable oil : a review of approaches , challenges , and opportunities,” *Renewable and Sustainable Energy Reviews.*, 146 111191 (2021). doi:10.1016/j.rser.2021.111191.

5) S. Syahrullail, M.A.M. Hariz, M.K.A. Hamid, and A.R.A. Bakar, “Friction characteristic of mineral oil containing palm fatty acid distillate using four ball tribo-tester,” *Procedia Engineering.*, 68 166–171 (2013). doi:10.1016/j.proeng.2013.12.163.

6) A.N. Afifah, S. Syahrullail, N.I. Wan Azlee, N.A. Che Sidik, W.J. Yahya, and E. Abd Rahim, “Biolubricant production from palm stearin through enzymatic transesterification method,” *Biochemical Engineering Journal.*, 148 178–184 (2019). doi:10.1016/j.bej.2019.05.009.

7) M. Fadzil, and A. Bahar, “Evaluation of crude fatty acids as lubricant,” *Journal of Biolubricant Engineering and Science.*, 2 (1) 1–6 (2020).

8) S.S.K. Kiu, S. Yusup, C.V. Soon, T. Arpin, S. Samion, and R.N.M. Kamil, “Tribological investigation of graphene as lubricant additive in vegetable oil,” *Journal of Physical Science.*, 28 257–267 (2017). doi:10.21315/jps2017.28.s1.17.

9) A.C. Opia, M. Kameil, A. Hamid, C.A.N. Johnson, A.B. Rahim, and M.B. Abdulrahman, “Nano-particles additives as a promising trend in tribology : a review on their fundamentals and mechanisms on friction and wear reduction ,” *EVERGREEN Joint Journal of Novel Carbon Resource Sciences & Green Asia Strategy.*, 08 (04) 777-798 (2021). doi.org/10.5109/4742121

10) S. Syahrullail, C.S.N. Azwadi, and T.C. Ing, “The metal flow evaluation of billet extruded with rbd palm stearin,” *International Review of Mechanical Engineering.*, 5 (2011).

11) N. Sapawe, S. Samion, P. Zulhanafi, C.S. Nor Azwadi, and M.F. Hanafi, “Effect of addition of tertiary-butyl hydroquinone into palm oil to reduce wear and friction using four-ball tribotester,” *Tribology Transactions.*, 59 (5) 883–888 (2016). doi:10.1080/10402004.2015.1118584.

12) N.F. Azman, and S. Samion, “Dispersion stability and lubrication mechanism of nanolubricants : a

review," *International Journal of Precision Engineering and Manufacturing-Green Technology.*, 6 (2) 393–414 (2019). doi:10.1007/s40684-019-00080-x.

13) A. Yahaya, S. Samion, and M.N. Musa, "Determination of friction coefficient in the lubricated ring upsetting with palm kernel oil for cold forging of aluminum alloys," *Jurnal Tribologi.*, 25 16–28 (2020).
14) I. Golshokouh, S. Syahrullail, F.N. Ani, and H.H. Masjuki, "Investigation of palm fatty acid distillate as an alternative lubricant of petrochemical based lubricants, tested at various speeds," *International Review of Mechanical Engineering.*, 7 (1) 72–80 (2013).
15) S. Syahrullail, S. Kamitani, and K. Nakanishi, "Experimental evaluation of refined, bleached, and deodorized palm olein and palm stearin in cold extrusion of aluminum a1050," *Tribology Transactions.*, 55 (2) 199–209 (2012). doi:10.1080/10402004.2011.648826.
16) M. Hassan, F.N. Ani, and S. Syahrullail, "Tribological performance of refined, bleached and deodorised palm olein blends bio-lubricants," *Journal of Oil Palm Research.*, 28 (4) 510–519 (2016). doi:10.21894/jopr.2016.2804.12.
17) S. Ahmad, R.N. Chendang, M.A. Lajis, A. Supawi, and E.A. Rahim, "Surface integrity of rbd palm oil as a bio degradable oil based dielectric fluid on sustainable electrical discharge machining (edm) of aisi d2 steel," *EVERGREEN Joint Journal of Novel Carbon Resource Sciences & Green Asia Strategy.*, 9 (1) 509–517 (2020). doi:10.1007/978-981-13-8297-0_53.
18) A. Kuncoro, and W.W. Purwanto, "Analysis of energy-water nexus palm oil biodiesel production in riau using life cycle assessment and water footprint methods," *EVERGREEN Joint Journal of Novel Carbon Resource Sciences & Green Asia Strategy.*, 7 (1) 104–110 (2020). doi:10.5109/2740965.
19) P. Zulhanafi, S. Syahrullail, and M.A. Ahmad, "The performances of palm mid olein as lubricant in journal bearing application," *Proceedings of Asia International Conference on Tribology 2018.*, 382–383 (2018).
20) P. Zulhanafi, S. Syahrullail, and M.A. Ahmad, "The tribological performance of hydrodynamic journal bearing using bio-based lubricant," *Tribology in Industry.*, 42 (2) 278–287 (2020). doi:10.24874/ti.843.02.20.05.
21) S. Matele, and K.N. Pandey, "Effect of surface texturing on the dynamic characteristics of hydrodynamic journal bearing comprising concepts of green tribology," *Proceedings of the Institution of Mechanical Engineers, Part J: Journal of Engineering Tribology.*, 232 (11) 1365–1376 (2018). doi:10.1177/1350650117752611.
22) B. Guo, "Optimal surface texture design of journal bearing with axial grooves," *International Journal of Heat and Technology.*, 35 (2) 267–272 (2017). doi:10.18280/ijht.350206.
23) J. Triyono, R. Rahajeng, and E. Surojo, "Surface modification and hardness behavior of aisi 304 as an artificial hip joint using ammonia and scallop shell powder as a nitriding agent," *EVERGREEN Joint Journal of Novel Carbon Resource Sciences & Green Asia Strategy.*, 8 (2) 335–343 (2021). doi:10.5109/4480714.
24) A.B. Shinde, and P.M. Pawar, "Effect of partial grooving on the performance of hydrodynamic journal bearing," *Industrial Lubrication and Tribology.*, 69 (4) 574–584 (2017). doi:10.1108/ILT-06-2016-0124.
25) N. Tala-Ighil, and M. Fillon, "Surface texturing effect comparative analysis in the hydrodynamic journal bearings," *Mechanics & Industry.*, 16 (3) 302 (2015). doi:10.1051/meca/2015001.
26) G. Jamwal, S. Sharma, and R.K. Awasthi, "The dynamic performance analysis of chevron shape textured hydrodynamic bearings," *Industrial Lubrication and Tribology.*, (2019). doi:10.1108/ilt-05-2019-0172.
27) X. Liang, Z. Liu, H. Wang, X. Zhou, and X. Zhou, "Hydrodynamic lubrication of partial textured sliding journal bearing based on three-dimensional cfd," *Industrial Lubrication and Tribology.*, 68 (1) 106–115 (2016). doi:10.1108/ILT-04-2015-0055.
28) Q. Lin, Q. Bao, K. Li, M.M. Khonsari, and H. Zhao, "An investigation into the transient behavior of journal bearing with surface texture based on fluid-structure interaction approach," *Tribology International.*, 118 246–255 (2018). doi:10.1016/j.triboint.2017.09.026.
29) Y. Changru, N. Takata, K. Thu, and T. Miyazaki, "How lubricant plays a role in the heat pump system," *EVERGREEN Joint Journal of Novel Carbon Resource Sciences & Green Asia Strategy.*, 8 (1) 198–203 (2021). doi:10.5109/4372279.
30) S. Sharma, G. Jamwal, and R.K. Awasthi, "Enhancement of steady state performance of hydrodynamic journal bearing using chevron-shaped surface texture," *Proceedings of the Institution of Mechanical Engineers, Part J: Journal of Engineering Tribology.*, 0 (0) 1–11 (2019). doi:10.1177/1350650119847369.
31) L. Galda, J. Sep, A. Olszewski, and T. Zochowski, "Experimental investigation into surface texture effect on journal bearings performance," *Tribology International.*, 372–384 (2019). doi:10.1016/j.triboint.2019.03.073.
32) H. Yamada, H. Taura, and S. Kaneko, "Numerical and experimental analyses of the dynamic characteristics of journal bearings with square dimples," *Journal of Tribology.*, 140 1–13 (2018).

doi:10.1115/1.4037151.

33) H. Yamada, H. Taura, and S. Kaneko, "Static characteristics of journal bearings with square dimples," *Journal of Tribology.*, 139 (5) (2017). doi:10.1115/1.4035778.
34) S. Sharma, G. Jamwal, and R.K. Awasthi, "Numerical study on steady state performance enhancement of partial textured hydrodynamic journal bearing," *Industrial Lubrication and Tribology.*, (2019). doi:10.1108/ILT-03-2019-0083.
35) Y. Mao, Y. Jianxi, X. Wenjing, and L. Yonggang, "Study on the influence of round pits arrangement patterns on tribological properties of journal bearings," *Industrial Lubrication and Tribology.*, 71 (7) 931–941 (2019). doi:10.1108/ilt-07-2018-0264.
36) K.M. Faez, S. Hamdavi, T.V.V.L.N. Rao, H.H. Ya, and N.M. Mohamed, "Performance analysis of grooved hydrodynamic journal bearing with multi-depth textured surface," *International Journal of Vehicle Structures and Systems.*, 10 (2) 142–145 (2018). doi:10.4273/ijvss.10.2.13.
37) B. Manser, I. Belaidi, A. Hamrani, S. Khelladi, and F. Bakir, "Performance of hydrodynamic journal bearing under the combined influence of textured surface and journal misalignment: a numerical survey," *Comptes Rendus - Mecanique.*, 347 (2) 141–165 (2019). doi:10.1016/j.crme.2018.11.002.
38) R. Yu, P. Li, and W. Chen, "Study of grease lubricated journal bearing with partial surface texture," *Industrial Lubrication and Tribology.*, 68 (2) 149–157 (2016). doi:10.1108/ILT-03-2015-0028.
39) F.M. Meng, L. Zhang, Y. Liu, and T.T. Li, "Effect of compound dimple on tribological performances of journal bearing," *Tribology International.*, 91 99–110 (2015). doi:10.1016/j.triboint.2015.06.030.
40) F.M. Meng, and W. Zhang, "Effects of compound groove texture on noise of journal bearing," *Journal of Tribology.*, 140 (3) 1–12 (2018). doi:10.1115/1.4038353.
41) H. Ambarita, M.R. Siregar, K. Kishinami, M. Daimaruya, and H. Kawai, "Application of cfd in indonesian research: a review," *Journal of Physics: Conference Series.*, 1005 (2018). doi:10.1088/1742-6596/1005/1/012014.
42) G. Gao, Z. Yin, D. Jiang, and X. Zhang, "Numerical analysis of plain journal bearing under hydrodynamic lubrication by water," *Tribology International.*, 75 31–38 (2014). doi:10.1016/j.triboint.2014.03.009.
43) Z. Rasep, M. Noor, A. Witri, M. Yazid, and S. Samion, "A study of cavitation effect in a journal bearing using cfd : a case study of engine oil , palm oil and water," *Jurnal Tribologi.*, 28 48–62 (2021).
44) P. Zulhanafi, "Tribological Performances of Journal Bearing Using Palm Oil Based Lubricant," Universiti Teknologi Malaysia, 2021.
45) S. Susilowati, F. Hilmy, D. Arfiandani, Muchammad, M. Tauviqirrahman, and J. Jamari, "Effect of eccentricity ratio on the hydrodynamic performance of journal bearing considering cavitation," *AIP Conference Proceedings.*, 2097 (2019). doi:10.1063/1.5098243.
46) P.D. Kalbande, D.Y. Dhande, and D.W. Pande, "CFD analysis of carbon fiber reinforced polytetrafluoroethylene (ptfe) hydrodynamic journal bearing using optimization technique," *International Conference on Automatic Control and Dynamic Optimization Techniques, ICACDOT 2016.*, 629–634 (2016). doi:10.1109/ICACDOT.2016.7877662.
47) N. Tala-Ighil, M. Fillon, and P. Maspeyrot, "Effect of textured area on the performances of a hydrodynamic journal bearing," *Tribology International.*, 44 (3) 211–219 (2011). doi:10.1016/j.triboint.2010.10.003.